Journal of Applied Spectroscopy, Vol. 78, No. 5, November, 2011 (Russian Original Vol. 78, No. 5, September–October, 2011)

QUASI-PHASE-MATCHED SUM-FREQUENCY GENERATION IN LAYERED STRUCTURES

R. J. Kasumova

UDC 535.3

A theory has been developed for quasi-phase-matched generation of a wave at a sum-frequency within a constant-intensity approximation. In contrast to a constant-field approximation, the constant-intensity approach has been found to give an optimum pump intensity value at which the conversion efficiency reaches its maximum. Analytical expressions have been derived for optimal values of the problem's parameters. Ways to enhance the power of the coherent optical radiation are shown and analyzed. This will make it possible, in particular, to increase the power in an RGB-source color for which the sum-frequency generation is responsible.

Keywords: *regular domain structures, constant-intensity approximation.*

Introduction. Intense coherent radiation in the frequency range from the IR to the UV spectral regions is currently produced using quasi-phase-matched interactions [1–4]. Simultaneous generation at several wavelengths is possible in regular domain structures (RDS) based on a single periodically poled crystal. This makes such multi-layer domain structures exceedingly interesting [5, 6]. Furthermore, ultrashort light pulses can be compressed by using aperiodically poled nonlinear crystals [7]. The pulse length was decreased by 150 times in a $LiNbO_3$ crystal with an aperiodic structure [8].

It is known that the energy of laser radiation can be transformed by using nonlinear optics and multiplication and mixing of optical frequencies. As a result, powerful sources of tuned coherent optical radiation can be obtained. In particular, IR radiation can be efficiently transformed into visible radiation by using sum-frequency generation. This type of frequency transformation is used rather often in layered structures. For example, blue light resulted from summation of the pump radiation (744 nm) and the laser line emission (1084 nm) with quasi-phase-matched interaction during sum-frequency generation [9]. The second section gave blue light (460 nm) by a sum-frequency shift of the pump and the idler wave obtained in the first section [10]. Radiation with λ = 1064 nm was transformed into visible radiation with λ = 611 nm [11].

RDS crystals are currently used successfully to produce RGB-sources [9–11]. Two basic light models that are used in modern industry and technology are known to exist. One model uses three colors (RGB: red, green, blue); the other, four (CMYK: cyan, magenta, yellow, black). The digital RGB model is used extensively in computer technology, in particular on the internet, and also to produce light images on computer monitors and cellular telephone displays. The CMYK model is used in graphic arts and color printers.

Generation of a sum-frequency and optical harmonics is currently used to obtain the three primary colors during the fabrication of high-powered quasi-CW RGB-sources. Several nonlinear crystals in which various nonlinear processes were carried out sequentially in order to obtain the three primary colors were used as quasi-pulsed high-powered RGB-sources in the initial development stage [6]. In contrast with the similar cascade transformation of frequency using a series of crystals, the next step became the fabrication of an RGB-source based on a single unique RDS-crystal in which quasi-phase-matched interaction of optical waves occurred. Aperiodic poled lithium niobate $LiNbO_3$ doped with Nd (Nd^{3+}) was used as the crystal. It was pumped by radiation from a pulsed titanium-sapphire laser with λ = 744 nm. The Nd ion emitted laser radiation with λ = 1084 and 1372 nm as a result of the stimulated transition. The aperiodic domain structure generated their second harmonics (green and red). The third color of the RGB-source, blue, was produced as a result of a sum-shift of the pump radiation with λ = 744 nm and the laser

Baku State University, 23 Acad. Z. Khalilov St., Baku, AZ1148, Azerbaijan; e-mail: rkasumova@azdata.net.
Translated from Zhurnal Prikladnoi Spektroskopii, Vol. 78, No. 5, pp. 707–715, September–October, 2011. Original article submitted April 19, 2011.

0021-9037/11/7805-0659

emission line with λ = 1084 nm [9]. Thus, generation at three frequencies without using additional nonlinear optical elements was achieved. Another version of an RGB-source was proposed [10] where a stoichiometric lithium tantalate crystal with two periods was pumped by a source with green light (532 nm) in order to generate red and blue light. The first section gave red light (631 nm) owing to optical parametric generation; the second section, blue light (460 nm) as the result of a sum-frequency shift of the pump radiation and the idler wave obtained in the first section. Several nonlinear optical processes were carried out simultaneously in an experiment with a single periodically poled crystal [11]. These included optical parametric generation, sum-frequency generation, and generation of the second and third harmonics. For this, a lithium niobate crystal with two grating periodicities of the nonlinear susceptibility modulation was used. Optical parametric generation of the signal wave with λ = 1.43 μm occurred in the first section. Red was produced by generation of the sum-frequency between the signal wave and the pump wave. Generation of the second and third harmonics occurred simultaneously in the second section. The resulting transformation efficiency was low. The researchers suggested ways to increase it that were based on an analysis for an unspent pump.

Theoretical analysis of quasi-phase-matched interaction is performed mainly in the constant-field approximation that does not take into account the reverse reaction of excited waves on the exciting wave. As a result, coherent lengths of layers-domains in this approximation have identical values whereas the frequency transformation efficiency increases smoothly with pump intensity and with increasing length of the nonlinear interaction.

Simultaneous consideration of phase changes and the losses of interacting waves can be achieved in the constant-intensity approximation [12]. The variable nature of the transformation efficiency as a function of pump intensity, phase mismatch, and layer lengths was found as the result of an analysis in this approximation. Furthermore, the dependence of the optimal parameter values at which the transformation efficiency is maximal on the losses of interacting waves was found in this approximation. Detailed analytical and numerical analyses of quasi-phase-matched interaction for the generation of second and third harmonics were carried out [13–15]. It was shown that selection of the optimal parameters can increase by several times the power of the harmonics. An analytical expression for the transverse dimension (length) of the fourth domain at which the maximum transformation of the signal-wave energy into energy of the sum-frequency wave occurs was derived for generation of the sum-frequency wave.

The goal of the present work was to investigate in further detail quasi-phase-matched generation of sum-frequency radiation in the constant-intensity approximation of the pump radiation. An analytical expression was obtained for the transformation efficiency for n domains. The pathways for increasing the transformation efficiency of the signal wave and, as a result, the power of the coherent optical radiation as a function of pump intensity and phase mismatch were analyzed in detail.

Theory. Let us examine nonlinear interaction in an RDS crystal during sum-frequency generation. We suppose that the structure is composed of n layers with inverted optical axes. First let us examine the mixing of optical frequencies in the first domain.

The interaction of three waves of frequencies $\omega_{1,2,3}$ ($\omega_3 = \omega_1 + \omega_2$) in a nonlinear dissipative and dispersive medium (in our instance, in the first domain) obeys the equations [15]:

$$\begin{aligned} dA_1/dz + \delta_1 A_1 &= -i\gamma_1 A_3 A_2^* \exp(i\Delta_1 z), \\ dA_2/dz + \delta_2 A_2 &= -i\gamma_2 A_3 A_2^* \exp(i\Delta_1 z), \\ dA_3/dz + \delta_3 A_2 &= -i\gamma_3 A_1 A_2^* \exp(i\Delta_1 z), \end{aligned} \tag{1}$$

where A_j are complex amplitudes of the signal ($j = 1$), pump ($j = 2$), and idler waves ($j = 3$) of frequencies ω_j; γ_j, coefficients of absorption and nonlinear coupling of the interacting waves of frequencies ω_j ($j = 1$–3); $\Delta_1 = k_3 - k_2 - k_1$, the phase mismatch in the first domain.

We solve system (1) during generation of the sum-frequency with boundary conditions at the entrance to the first domain

$$A_{1,2}(z=0) = A_{10,20}\exp(i\phi_{10,20}), \quad A_3(z=0) = 0. \tag{2}$$

Here $z = 0$ corresponds to the entrance to the first domain and $\phi_{10,20}$, the initial phase of the signal wave and pump wave at the entrance to the first domain.

Let us use the standard method for calculating quasi-phase-matched interaction in the constant-intensity approximation developed before [13]. By solving system (1) in the constant-intensity approximation with the conditions of Eq. (2), we obtain the following expression for the complex amplitude of the idler wave at the exit of the domain ($z = l_1$) [16, 17]:

$$A_3(l_1) = -i\gamma_3 A_{10} A_{20} l_1 \operatorname{sinc}(\lambda_1' l_1) \exp[i\phi_{10} + i\phi_{20} - (\delta_1 + \delta_2 + \delta_3 + i\Delta_1) l_1/2], \tag{3}$$

where

$$\lambda_1' = \sqrt{\Gamma_1^2 + \Gamma_2^2 - \frac{(\delta_3 - \delta_1 - \delta_2 - i\Delta_1)^2}{4}}, \quad \Gamma_1^2 = \gamma_2\gamma_3 I_{10}, \quad \Gamma_2^2 = \gamma_1\gamma_3 I_{20},$$

$$\operatorname{sinc} x = \sin x/x, \quad I_j = A_j A_j^*.$$

The coherent length of the first domain, i.e., the optimal domain length that provides the maximum amplitude of the sum-frequency wave, is determined from Eq. (3):

$$l_{1\text{opt}} = \pi \Big/ 2\sqrt{\Gamma_1^2 + \Gamma_2^2 - \frac{(\delta_3 - \delta_1 - \delta_2 - i\Delta_1)^2}{4}}. \tag{4}$$

It follows from Eq. (4) that the coherent length depends on the intensities of the pump wave I_{20} and signal wave I_{10} and the phase mismatch and losses in the first domain. If the relationship $\delta_3 = \delta_1 + \delta_2$ is fulfilled, then Eq. (4) transforms into

$$l_{1\text{opt}}' = [\arctan(\lambda_1/\delta_3)]/\lambda_1, \tag{5}$$

where $\lambda_1 = \sqrt{\Gamma_1^2 + \Gamma_2^2 + \Delta_1^2/4}$.

For small losses, setting $\delta_j = 0$ in Eq. (4), we obtain a simpler expression for the optimal domain length

$$l_{1\text{opt}} = \pi \Big/ \left[2\sqrt{\Gamma_1^2 + \Gamma_2^2 + \Delta_1^2/4}\right].$$

It can be seen that, in contrast with the result in the constant-field approximation, $l_{1\ \text{opt}}$ depends also on parameter Γ_1 (because $\gamma_2 \neq 0$ in the examined approximation). The coherent domain length decreases as I_{10}, I_{20}, and Δ_1 increase.

The quadratic susceptibility tensor changes to the opposite sign in the second layer. The quantities δ_j', γ_j' ($\gamma_j' = -\gamma_j$), and Δ_2 determine the losses and nonlinear coefficients of coupling and phase mismatch in this domain, respectively.

The boundary conditions at the entrance to the second domain are:

$$A_j(z=0) = A_j(l_1) \exp[i\phi_j(l_1)], \quad j = 1\text{–}3, \tag{6}$$

where $\phi_j(l_1)$ is the phase progression at the boundary of the layers of frequency ω_j. Here $z = 0$ now determines the entrance to the second domain.

We use the standard method to solve system (1) with boundary conditions for this layer and obtain for the complex amplitude of the idler wave at the exit of the second domain:

$$A_3(l_2) = A_3(l_1) \exp\left[-\frac{\delta_1' + \delta_2' + \delta_3' + i\Delta_2}{2} l_2 + i\phi_3(l_1)\right]$$

$$\times\left\{\cos\lambda_2' l_2 + \left[-i\gamma_3' \frac{A_1(l_1) A_2(l_1)}{A_3(l_1)} e^{i[\phi_1(l_1) + \phi_2(l_1) - \phi_3(l_1)]} + \frac{\delta_1' + \delta_2' - \delta_3' + i\Delta_2}{2}\right] \frac{\sin\lambda_2' l_2}{\lambda_2'}\right\}, \tag{7}$$

where

$$\lambda_2' = \sqrt{\Gamma_1'^2 + \Gamma_2'^2 - \frac{(\delta_3' - \delta_1' - \delta_2' - i\Delta_1)^2}{4}}\ ,\quad \Gamma_1'^2 = \gamma_2'\gamma_3' I_1(l_1),\quad \Gamma_2'^2 = \gamma_1'\gamma_3' I_2(l_1)\ .$$

We obtain from Eq. (7) the following expression for the optimal length of the second layer

$$l_{2\text{opt}} = \pi \Big/ \sqrt{\Gamma_1'^2 + \Gamma_2'^2 - (\delta_3' - \delta_1' - \delta_2' - i\Delta_1)^2/4}\ . \tag{8}$$

It follows from the analysis that whereas energy of the signal wave in the first layer converted into energy of the sum-frequency wave, the reverse transformation of energy of the sum-frequency wave into energy of the signal wave occurred in the second layer at the optimal layer lengths with identical orientations of the crystal layers. The transformation efficiency increases gradually from layer to layer in our instance of inverted layers. This was examined in detail before [13]. An analysis of Eq. (7) also shows that there are optimal phase mismatches Δ_k, k = 1, 2, at which the transformation efficiency is greatest.

The wave phase-jump constants at the entrance to the first domain ϕ_{10}, to the second domain $\phi_{1,2}(l_1)$, and also phase-jump constants at the boundaries of the second-third and third-fourth domains are omitted in subsequent analytical expressions in order to avoid unwieldy formulas. However, these phase-jumps are taken into account in analyzing the transformation process in RDSs.

Analogously to the calculation performed for the preceding layer, the following expression can be obtained for the complex amplitude of the sum-frequency wave (i.e., the idler wave) at the exit of the third domain

$$A_3(l_3) = A_3(l_2)\exp\left(-\frac{\delta_1'' + \delta_2'' + \delta_3'' + i\Delta_3}{2} l_3\right)\left\{\cos\lambda_3' l_3 + \left[-i\gamma_3''\frac{A_1(l_2)\,A_2(l_2)}{A_3(l_2)} + \frac{\delta_1'' + \delta_2'' - \delta_3'' + i\Delta_3}{2}\right]\frac{\sin\lambda_3' l_3}{\lambda_3'}\right\}, \tag{9}$$

where

$$\lambda_3'' = \sqrt{\Gamma_1''^2 + \Gamma_2''^2 - \frac{(\delta_3'' - \delta_1'' - \delta_2'' - i\Delta_3)^2}{4}}\ ,\quad \Gamma_1''^2 = \gamma_2''\gamma_3'' I_1(l_2),\quad \Gamma_2''^2 = \gamma_1''\gamma_3'' I_2(l_2)\ .$$

The following designations are used for this layer: δ_j'' are the losses; $\gamma_j'' = \gamma_j$, coefficients of nonlinear coupling of the interacting waves; Δ_3, the phase mismatch. The expression for the complex amplitude of the idler wave at the exit of the fourth domain is:

$$\begin{aligned} A_3(l_4) &= A_3(l_3)\exp\left(-\frac{\delta_1''' + \delta_2''' + \delta_3''' + i\Delta_4}{2} l_4\right) \\ &\times\left\{\cos\lambda_4' l_4 + \left[-i\gamma_3'''\frac{A_1(l_3)\,A_2(l_2)}{A_3(l_3)} + \frac{\delta_1''' + \delta_2''' - \delta_3''' + i\Delta_4}{2}\right]\frac{\sin\lambda_4' l_4}{\lambda_4'}\right\}, \end{aligned} \tag{10}$$

where

$$\lambda_4' = \sqrt{\Gamma_1'''^2 + \Gamma_2'''^2 - \frac{(\delta_3''' - \delta_1''' - \delta_2''' - i\Delta_4)^2}{4}}\ ,\quad \Gamma_1'''^2 = \gamma_2'''\gamma_3''' I_1(l_3),\quad \Gamma_2'''^2 = \gamma_1'''\gamma_3''' I_2(l_3)\ .$$

Here the following designations are used: δ_j''' are the losses; $\gamma_j''' = -\gamma_j$, coefficients of the interacting waves; Δ_4, the phase mismatch.

Finally, for n domains, we obtain:

$$A_3(l_n) = A_3(l_{n-1}) \exp\left(-\frac{\delta_1 + \delta_2 + \delta_3 + i\Delta_n}{2} l_n\right)$$

$$\times\left\{\cos\lambda_n' l_n + \left[-i\gamma_3 \frac{A_1(l_{n-1})\, A_2(l_{n-1})}{A_3(l_{n-1})} + \frac{\delta_1 + \delta_2 - \delta_3 + i\Delta_n}{2}\right] \frac{\sin\lambda_n' l_n}{\lambda_n'}\right\}, \tag{11}$$

where

$$\lambda_n' = \sqrt{\Gamma_1^2 + \Gamma_2^2 - \frac{(\delta_3 - \delta_1 - \delta_2 - i\Delta_n)^2}{4}}\ , \quad \Gamma_1^2 = \gamma_2\gamma_3 I_1(l_{n-1}),\ \ \Gamma_2^2 = \gamma_1\gamma_3 I_2(l_{n-1})\ ,$$

δ_j are the losses; γ_j, coefficients of nonlinear coupling of the interacting waves ($\gamma_j = -\gamma_j$ for n even and $\gamma_j = \gamma_j$ for n odd); Δ_n, the phase mismatch.

Further analysis of the three-frequency interaction was performed under the conditions used in RGB-sources [9–11]. In this instance, one powerful and one weak optical wave is present at the entrance into the structure, i.e., high-intensity pumping where $I_{20} >> I_{10}$. Therefore, the energy transfer during generation of the sum-frequency occurs mainly between the signal and generated (idler) waves. Then the intensity of the pump wave can be considered practically constant, i.e., the relationship $I_2(z = 0) = I_2(l_1) = I_2(l_2) = I_2(l_3) = I_2(l_4)$ is fulfilled.

The coherent length of the n-th domain obeys the following expression in an RDS-crystal composed of layers-domains with identical nonlinear coefficients:

$$l_{n\,\mathrm{opt}} = \pi \Big/ 2\sqrt{\Gamma_2^2 - \frac{(\delta_3 - \delta_1 - \delta_2 - i\Delta_n)^2}{4}}\ . \tag{12}$$

It can be seen that the coherent lengths of the domains are different for different phase mismatches and losses in the domains.

Let us introduce the concept of the transformation efficiency along the signal wave: $\eta_3(l_k) = I_3(l_k)/I_{10}$, $k = 1$–n. Let us examine the generation of the sum-frequency in an RDS-crystal with identical phase mismatches in each of the domains ($\Delta_k = \Delta$, $k = 1$–4) and the optimal domain lengths, where $l_{k\,\mathrm{opt}}$ is determined from the condition $\lambda_k l_{k\,\mathrm{opt}} = \pi/2$. We obtain from Eq. (7) with the imposed conditions for the transformation efficiency at the exit of the second domain ($\delta_3 = \delta_1 + \delta_2$):

$$\eta_3(l_2) = \eta_3(l_{1\mathrm{opt}}) \exp(-2\delta_3 l_2)\left[\cos^2\lambda_2 l_2 + (\Delta/\lambda_2)^2 \sin^2\lambda_2 l_2\right], \tag{13}$$

where $\lambda_2 = \sqrt{\Gamma_2^2 + \Delta^2/4}$, $\Gamma_2^2 = \gamma_1\gamma_3 I_{20}$,

$$\eta_3(l_1) = I_3(l_1)/I_{10} = \gamma_3^2 I_{20} l_1^2\, \mathrm{sinc}^2(\tilde{\lambda}_1 l_1) \exp(-2\delta_3 l_1)\ , \quad \tilde{\lambda}_1 = \sqrt{\Gamma_2^2 + \Delta^2/4}\ .$$

We have from Eq. (9) at the exit of the third domain

$$\eta_3(l_3) = \eta_3(l_{2\mathrm{opt}}) \exp(-2\delta_3 l_3)\left[\cos^2\lambda_3 l_3 + \left(\Delta - \lambda_2^2/\Delta\right)^2 \frac{\sin^2\lambda_3 l_3}{\lambda_3^2}\right], \tag{14}$$

where $\lambda_3 = \sqrt{\Gamma_2^2 + \Delta^2/4}$. We obtain from Eq. (10) at the exit of the fourth domain

$$\eta_3(l_4) = \eta_3(l_{3\mathrm{opt}}) \exp(-2\delta_3 l_4)\left[\cos^2\lambda_4 l_4 + \left(\Delta - \frac{\lambda_3^2}{\Delta - \lambda_2^2/\Delta}\right) \frac{\sin^2\lambda_4 l_4}{\lambda_4^2}\right], \tag{15}$$

where $\lambda_4 = \sqrt{\Gamma_2^2 + \Delta^2/4}$ ..

It can be seen from Eqs. (13)–(15) that $\lambda_1 = \lambda_2 = \lambda_3 = \lambda_4 = \lambda$ under the examined analytical conditions. Let us introduce parameter $R = \Delta/\lambda$. Then the expressions for the transformation efficiency in each layer become

$$\eta_3 (l_{1\text{opt}}) = (1 - R^2/4) \exp (-2\delta_3 l_{1\text{opt}}) ,$$

$$\eta_3 (l_2) = \eta_3 (l_{1\text{opt}}) \exp (-2\delta_3 l_2) [\cos^2 \lambda_2 l_2 + R^2 \sin^2 \lambda_2 l_2] ,$$

$$\eta_3 (l_3) = \eta_3 (l_{2\text{opt}}) \exp (-2\delta_3 l_3) [\cos^2 \lambda_3 l_3 + (R - 1/R)^2 \sin^2 \lambda_3 l_3] ,$$

$$\eta_3 (l_4) = \eta_3 (l_{3\text{opt}}) \exp (-2\delta_3 l_4) \left[\cos^2 \lambda_4 l_4 + \left(R - \frac{1}{R - 1/R}\right)^2 \sin^2 \lambda_4 l_4\right] .$$

The transformation efficiency of signal-wave energy into the sum-frequency wave after the fourth domain with $l_4 = l_4$ opt is:

$$\eta_3 (l_{4\text{opt}}) = \exp (-2\delta_3 l_{\text{opt}} 4) \left(1 - \frac{R^2}{4}\right) R^2 \left(R - \frac{1}{R}\right)^2 \left(R - \frac{1}{R - 1/R}\right)^2 . \quad (16)$$

The resulting transformation efficiency $\eta_3(l_{4\ \text{opt}})$ is expressed through serial fractions [18]. The expression for the transformation efficiency for any finite number of domains $\eta_3(l_{n\ \text{opt}})$ can be written analogously. For example, we have after six domains

$$\eta_3 (l_{6\text{opt}}) = \exp (-2\delta_3 l_{\text{opt}} 6) (1 - R^2/4)$$

$$\times R^2 \left(R - \frac{1}{R}\right)^2 \left(R - \frac{1}{R - \frac{1}{R}}\right)^2 \left(R - \frac{1}{R - \frac{1}{R - 1/R}}\right)^2 \left(R - \frac{1}{R - \frac{1}{R - 1/(R - 1/R)}}\right)^2 . \quad (17)$$

We determine the value of R at which $\eta_3(l_{4\ \text{opt}})$ is maximum analytically from Eq. (16): $R_{\text{opt}} = 1.8478$. If losses are ignored ($\delta_3 = 0$), then the transformation efficiency for R_{opt} attains the following values: $\eta_3(l_{1\ \text{opt}}) = 0.1449$; $\eta_3(l_{2\ \text{opt}}) = 0.4947$; $\eta_3(l_{3\ \text{opt}}) = 0.8445$; $\eta_3(l_{4\ \text{opt}}) = 0.9894$. The transformation efficiency is already significant (almost 100%) after a small number (four) of domains. This means that the energy of the signal wave was practically completely transferred into energy of the sum-frequency wave. Therefore, high values of ?3 can be obtained without resorting to a large number of layers-domains.

Discussion. Figures 1–3 show results of numerical calculations using analytical expressions Eqs. (13)–(15) that were obtained in the constant-intensity approximation for generation of the sum-frequency. Figure 1 shows the transformation efficiency into the sum-frequency $\eta_3(l_k) = I_3(l_k)/I_{10}$ as a function of the given lengths of the first, second, third, and fourth domains l_k' ($l_k' = \Gamma_2 l_k$, k = 1–4). The analysis showed that the curvature of the curves decreased with an increasing number of layers-domains whereas the efficiency increased and reached practically 100% at the determined optimal parameters. This indicated that the energy of the signal wave was fully transformed into energy of the sum-frequency wave. A comparison of the corresponding solid and dash-dot curves showed that both the transformation efficiency $\eta_3(l_j)$ and the optimal domain lengths decreased as the losses increased. This resulted in the corresponding dash-dot curves being displaced to the right of the solid curves.

Figure 2 shows the transformation efficiency in four domains $\eta_3(l_4)$ as a function of the given phase mismatch $\Delta' = \Delta/2\Gamma_2$. Energy of the signal wave was transferred gradually into energy of the sum-frequency wave within a domain. The curves differed in the sizes of the losses. Each curve reached a maximum at its own value of the optimal phase mismatch $\Delta_{k\ \text{opt}}$. A well-known decrease of transformation efficiency in addition to an increase of the optimal value of the given phase mismatch were observed as the losses increased. This shifted the curves to the right (curves 1–3). Further analysis showed that the optimal value of the phase mismatch $\Delta_{j\ \text{opt}}$ increased as the number of

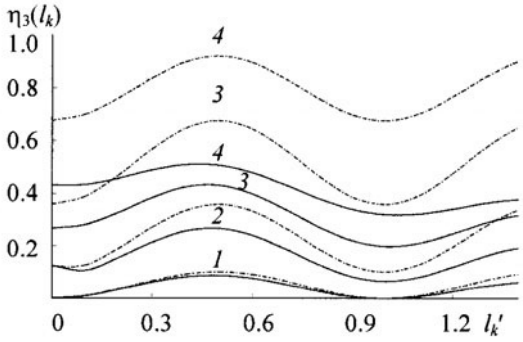

Fig. 1. Transformation efficiency to sum-frequency $\eta_3(l_k) = I_3(l_k)/I_0$ as a function of given domain lengths $l'_{1,2,3,4} = \Gamma_2 l_k$, k = 1–4 calculated in the constant-intensity approximation for $\Delta' = \Delta/2\Gamma_2 = 3$ for $\delta_3 = \delta_1 + \delta_2$, $\delta'_3 = \delta_3/\Gamma_2 = 0$ (dashed lines) and 0.15 (solid lines); $\lambda_k l_{k\,\mathrm{opt}} = \pi/2$.

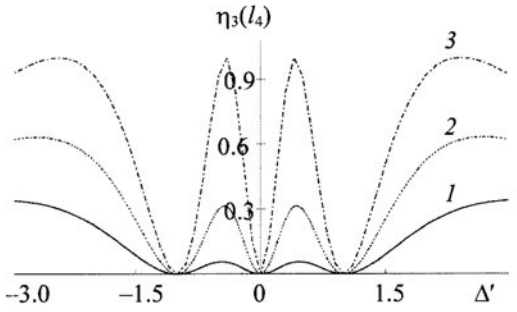

Fig. 2. The quantities $\eta_3(l_4)$ as functions of given phase mismatch $\Delta' = \Delta/2\Gamma_2$ calculated in the constant-intensity approximation for the optimal domain lengths; $\lambda_k l_{k\,\mathrm{opt}} = \pi/2$; $\delta_3 = \delta_1 + \delta_2$, $\delta'_3 = 0$ (1), 0.1 (2), and 0.25 (3).

domains increased, i.e., the relationship $\Delta_{1\ \mathrm{opt}} < \Delta_{2\ \mathrm{opt}} < \Delta_{3\ \mathrm{opt}} < \Delta_{4\ \mathrm{opt}}$ was fulfilled, in analogy to the instance of harmonic generation [13, 14].

Figure 3 plots the behavior of the transformation efficiency $\eta_3(l_4)$ as a function of the given pump intensity $I'_2 = \Gamma_2 l_4$ for two values of the losses. It can be seen that the dependence is nonmonotonic, in contrast with the result obtained in the constant-field approximation. The existence of an optimal pump intensity was also confirmed experimentally by studying nonlinear interaction of optical waves [19]. The optimal pump intensity was markedly reduced upon doubling the decay of the interacting waves in a nonlinear medium.

A numerical estimate of the expected transformation power into the three colors of an RGB-source under the published experimental conditions [11] was carried out based on an analysis in the constant-intensity approximation. A $LiNbO_3$ crystal was used as the RDS-crystal. Two different nonlinear gratings that were situated one after the other were located within it. The pump wave was radiation from a Nd:YAG laser with gain modulation (pulse length 7 ns, λ = 1.064 μm).

The numerical calculation using the analytical expressions for the optimal lengths of four domains and transformation efficiencies was carried out for pump-radiation energy 2.2 mJ. The following optimal values of domain lengths were obtained for green light using results of the constant-intensity approximation with generation of the second harmonic [14] taking into account phase matching [11]: $l_{1\ \mathrm{opt}} = 11.14$ μm; $l_{2\ \mathrm{opt}} = 11.4975$; $l_{3\ \mathrm{opt}} = 12.44$; $l_{4\ \mathrm{opt}} = 13.266$. Hence, the grating dimension $l_{1\ \mathrm{opt}} + l_{2\ \mathrm{opt}} + l_{3\ \mathrm{opt}} + l_{4\ \mathrm{opt}} = 48.344$ μm. In this instance, the maximum energy of green light can reach ≈0.5 mJ. The results were used to estimate the optimum sum-frequency generation of red and

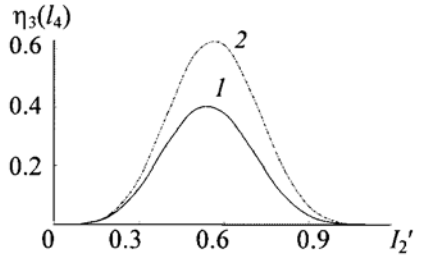

Fig. 3. The quantities $\eta_3(l_4)$ as functions of given pump intensity $I_2' = \Gamma_2 l_4$ calculated in the constant-intensity approximation for the optimal domain lengths; $\lambda_k l_{k\,\mathrm{opt}} = \pi/2$, $\Delta' = 2.5$, $\delta_3 = \delta_1 + \delta_2$, $\delta_3' = 0.1$ (2) and 0.2 (1).

blue light with cascade generation of the third harmonic of the signal wave. The maximum energy of red light with coherent domain lengths $l_{j\,\mathrm{opt}} = 10.4$ μm was 85 μJ. It was close to 17 μJ for $l_{j\,\mathrm{opt}} = 52$ μm for blue light. The analysis showed that the radiation energy in the colors of the RGB-source fell by an average of 20% if absorption in the domains was taken into account ($\delta_j/\Gamma_{1,2} = 0.15$–$0.20$). It is noteworthy that the given radiation energies were not obtained at the optimal pump intensity and phase mismatch in the crystal. Two nonlinear gratings with periodicities 27.6 and 15.2 μm in the crystal were used in the previous work [11]. The energy of blue light was 3.5 μJ; red, 1.8 μJ; green, 1.7 μJ.

Thus, according to the published scheme [11], the masks used to form a section with the appropriate domain structure can be altered using previous results [13] for each actual experiment (pump intensity, phase match, losses in layers) in order to increase the power of green light. Theoretical predictions of the coherent layer lengths for generation of the second harmonic of the pump and signal waves (for n layers) can be used to select similar values and to fabricate several pairs of masks for sections with small domain length fluctuations. Masks used to form the sections can be prepared according to the values calculated herein to generate the sum-frequency for n layers also wih small domain length fluctuations in order to incease the power in the red and blue light. Then, by preparing samples with several pairs of periodicities in both sections, the values of which change little from the theoretically predicted one, the best pair among them can be identified by direct experiments.

If the change of optimal domain lengths as a function of the change in the number of layers can be found theoretically, as follows from an analysis in the constant-intensity approximation, then the power of RGB-sources can be further increased. Use of the optimal pump intensity and phase mismatch between the interacting waves in addition to coherent domain lengths would also increase the power of the output radiation in the three colors.

Conclusion. The developed analytical method for frequency shifts in an RDS can be applied to the analysis of an intracavity parametric quasi-phase-matched interaction of optical waves. In particular, this enabled the power in the colors of an RGB-source that are due to generation of a sum-frequency to be increased. Recommendations are given for developing domain structures with the optimal parameters.

Acknowledgments. The work was supported financially by the Foundation for Science Development of the Azerbaijan Republic President (Grant No. EIF-2010-1(1)-40/14-M-9).

REFERENCES

1. A. Paul, R. A. Bartels, R. Tobey, H. Green, S. Weiman, I. P. Christov, M. M. Murnane, H. C. Kapteyn, and S. Backus, *Lett. Nature*, **421**, 51–54 (2000).
2. A. S. Chirkin, V. V. Volkov, G. D. Laptev, and E. Yu. Morozov, *Kvantovaya Élektron. (Moscow)*, **30**, 847–858 (2000).
3. M. M. Fejer, G. A. Magel, D. H. Jundt, and R. L. Byer, *IEEE J. Quantum Electron*., **28**, 2631–2654 (1992).
4. L. E. Myers, R. C. Eckardt, M. M. Fejer, R. L. Byer, W. R. Rosenberg, and J. W. Pierce, *J. Opt. Soc. Am. B: Opt. Phys*., **12**, 2102–2116 (1995).

5. O. Pfister, J. S. Wells, L. Hollberg, L. Zink, D. A. Van Baak, M. D. Levenson, and W. R. Bozenberg, *Opt. Lett.*, **22**, 1211–1214 (1997).
6. F. Brunner, E. Innerhofer, S. V. Marchese, T. Sudmeyer, R. Paschotta, T. Usami, H. Ito, S. Kurimura, K. Kitamura, G. Arisholm, and U. Keller, *Opt. Lett*., **29**, 1921–1923 (2004).
7. E. Yu. Morozov and A. S. Chirkin, *Kvantovaya Élektron. (Moscow)*, **34**, 227–232 (2004).
8. M. A. Arbore, A. Galvanauskas, D. Harter, M. H. Chou, and M. M. Fejer, *Opt. Lett.*, **22**, 1341–1344 (1997).
9. J. Capmany, *Appl. Phys. Lett*., **78**, 144–146 (2001).
10. Z. W. Liu, S. N. Zhu, Y. Y. Zhu, H. Liu, Y. Q. Lu, H. T. Wang, N. B. Ming, X. Y. Liang, and Z. Y. Xu, *Solid State Commun*., **119**, 363–366 (2001).
11. R. S. Cudney, M. Robles-Agudo, and L. A. Rios, *Opt. Express*, **14**, 10663–10668 (2006).
12. Z. H. Tagiev, R. J. Kasumova, R. A. Salmanova, and N. V. Kerimova, *J. Opt. B: Quantum Semiclassical Opt*., **3**, 84–87 (2001).
13. Z. H. Tagiev and R. J. Kasumova, *Opt. Commun*., **281**, 814–823 (2008).
14. R. J. Kasumova, G. A. Safarova, and M. A. Mamedov, in: *Materials of a Scientific Conference Dedicated to the 85th Birthday of G. Aliev* [in Russian], Baku, May 7–8, 2008, Izd. Baku Gos. Univ. (2008), 478–479.
15. R. J. Kasumova and A. Karimi, *Zh. Prikl. Spektrosk*., **77**, No. 1, 153–156 (2010).
16. Z. A. Tagiev, R. J. Kasumova, R. A. Salmanova, and N. V. Kerimova, *Vestn. Beloruss. Gos. Univ., Ser. Fiz. Mat. Nauk*, No. 3, 21–28 (2000).
17. Z. A. Tagiev, *Kvantovaya Élektron. (Moscow)*, **18**, 430–432 (1991).
18. H. Batteman and A. Erdelyi, *Higher Transcendental Functions*, McGraw-Hill Book Co., Inc., New York (1953), 2.
19. V. M. Gordienko, S. S. Grechin, A. A. Ivanov, and A. A. Podshivalov, *Kvantovaya Élektron. (Moscow)*, **35**, 525–526 (2005).